Journal of Molecular Liquids 268 (2018) 903–910

Contents lists available at ScienceDirect

Journal of Molecular Liquids

journal homepage: www.elsevier.com/locate/molliq

Structure and slow dynamics of protein hydration water

Gaia Camisasca[1], Antonio Iorio, Margherita De Marzio, Paola Gallo*

Dipartimento di Matematica e Fisica, Università Roma Tre, Via della Vasca Navale 84, Roma 00146, Italy

ARTICLE INFO

Article history:
Received 5 April 2018
Received in revised form 25 June 2018
Accepted 27 July 2018
Available online 2 August 2018

Keywords:
Hydration water
Hopping
Protein
Structure
Hydrogen bonds

ABSTRACT

We report results on the structure, local order and dynamics of water surrounding a lysozyme protein. The local order of water molecules is as much tetrahedral as in bulk water already at close vicinity of the protein but the number of hydrogen bonds depends more on the distance from the protein and gradually recovers bulk value upon moving outer. The dynamics of water seems in general to be more affected than its structure by the presence of the protein. An extremely long-relaxation detected in hydration water appears in the first monolayer around the protein, and the slow down is enhanced at low temperature. The dynamics of water within a layer of thickness 6 Å is sub-diffusive up to about ~1 ns, above 1 ns we observe a crossover toward a hopping regime over a length-scale larger than that of nearest neighbors molecules. This hopping seems connected to transient trapping of water molecules on some specific protein domains.

1. Introduction

The first layers of water surrounding proteins play a crucial role for their biological activity [1]. For this reason a huge amount of theoretical and experimental work [2-10] have been done to elucidate the physical properties of this kind of hydration water. These properties pertain the structure, the hydrogen (H) bonds and the dynamics of hydration water.

The three dimensional H-bond pattern of water is disrupted at the protein surface [11]. Hydration water can in fact bind or not to the protein, and if it does, depending on the hydrophilicity of the surface patches of the protein, it does via H-bonds. The number of water molecules engaged in protein-water H-bonds is linearly dependent on the temperature and experiences an abrupt increase of the slope in the supercooled regime [5]. It is worth mentioning that upon supercooling the protein undergoes the so-called protein dynamical transition [12,13], connected to the behavior of the mean square fluctuations of the protein itself [14]. Concerning water-water H-bonds, it has been shown that hydration water is able to form a two dimensional H-bond network around the protein and the stability of this network depends on the specific protein residue [15].

Hydration water experiences perturbations also from the dynamical point of view. Evidences of two distinct long relaxation times have been found experimentally [16-20]. The translational motion is slowed down with respect to bulk water already at ambient conditions and whereas bulk water shows a single structural α-relaxation, hydration water shows also in simulations two distinct structural relaxations [21-23]. One is the α-relaxation typical of many glass formers [12,24]. The other, the long-relaxation, is characterized by a longer relaxation time and an higher stretching character with respect to the α-relaxation [21-23]. The two relaxations show different temperature behavior. The α-relaxation of hydration water shows upon cooling a fragile-to-strong crossover like in bulk water [12,24]. while the dynamics of the long-relaxation, coupled to protein internal dynamics, shows a strong-to-strong crossover upon cooling and this occurs at the protein dynamical transition [14], therefore at higher temperature than the fragile-to-strong transition of the α-relaxation [23].

In this work we analyze the structure of hydration water in different layers around the protein and characterize its hydrogen bonding behavior. We also show the translational dynamics in a particular layer of thickness 6 Å which corresponds to a double molecular layer of water around the lysozyme. We analyze the dynamics by means of density self correlation functions in the ($\mathbf{r}$,t) and in the ($\mathbf{q}$,t) space to access to complementary information. These functions are respectively called the Self van Hove Function and the Self Intermediate Scattering Function.

The work is organized as follows: we describe in Section 2 the simulation methods and in Section 3 the investigated protein system. In Section 4 we present the results obtained probing the structure of hydration water and its hydrogen bond network. Section 5 is devoted to results on the dynamics, where we first present Self Intermediate Scattering Function and then Self van Hove Functions of hydration

* Corresponding author.
E-mail address: gallop@fis.uniroma3.it (P. Gallo).
[1] Present affiliation: Physics Department, Stockholm University, Sweden.

https://doi.org/10.1016/j.molliq.2018.07.104
0167-7322/

and bulk water. In Section 6 we draw our conclusion and discuss future directions.

2. Methods

A lysozyme protein immersed in water was simulated through classical Molecular dynamics (MD) all-atoms simulations. The cubic simulation box contains 1 lysozyme protein, 13982 water molecules and 8 Cl^- ions to maintain the total charge neutrality.

Protein interactions were described by the CHARMM force field [25,26] and water was modeled by the SPC/E potential [27]. The cutoff radius for the non-bonded van der Waals interactions was set to 10 Å. The Particle Mesh Ewald algorithm was used for the electrostatic interactions. Equations of motion were integrated with a time step of 1 fs. Equilibration runs were performed in the NPT ensamble for 30 ns at $T = 300$ K and 40 ns at $T = 250$ K. Both pressure and temperature were controlled using weak coupling algorithms [28]. Pressure is fixed at 1 bar. Then we execute production runs of 10 ns for analyzing the structure and further 20 ns for the dynamics. The frequency of coordinates storage is 500 fs and 1 fs respectively. Molecular dynamics simulations were also performed using the SPC/E water model on a box composed of 500 molecules in similar conditions. The Gromacs 4.5.5 [29] simulation package was used for all trajectories. Details on the protocol used to construct the simulation box can be found in Ref. [22].

3. Lysozyme and its hydration water

The lysozyme is an antimicrobial enzyme consisting of 129 amino acid residues having a molecular weight of 14.4 kDa. It folds into a compact globular structure having an ellipsoidal shape with dimensions $a \times c \times c = 2.25 \times 1.3 \times 1.3$ nm. The active site of lysozyme consists of a deep crevice, which divides the protein into two domains linked by an alpha helix. One domain consists almost entirely of beta-sheet structures, while the other domain is predominantly alpha-helical [30]. Our lysozyme is shown in Fig. 1, where we colored it according to the hydrophobicity/hydrophilicity of its residues. Note how hydrophobic sites are in general located more in the internal part of the protein, and this is very common for small globular proteins.

The structural organization of water around a protein is intimately related to the kind of protein sites that it is close to. A powerful tool to probe the local organization of water molecules around selected protein sites is the Radial Distribution Function (RDF). We calculated the RDF for the oxygen atoms of water with respect to a heavy atom of the protein. In Fig. 2 the RDFs calculated for the two extreme cases observed in our system are presented, namely curves that show two peaks within 6 Å from the protein heavy atom and curves that don't. In the example of the hydrated site we chose a surface site, therefore the protein atom is exposed to water. In this case water molecules organize around the site, creating correlation shells resembling the order of bulk water. Differently, when we selected a buried site the RDF shows a depletion region which extends outer up to about 6 Å, and where the probability of finding water molecules is very low.

From these RDFs we can see that considering water within 4 Å and 6 Å from the protein corresponds to analyze the behavior of the first layer and the first plus the second layers around the protein respectively. We will refer to this water as hydration water.

In Table 1 we report the number of water molecules that reside on average in the various investigated layers for two temperatures of our system, $T = 300$ K and $T = 250$ K. We consider a water molecule inside the layer $(r_1 - r_2)$ when the oxygen atom is located at a distance d such that $r_1 \leq d \leq r_2$ from the closest lysozyme atom.

4. Tetrahedrality and hydrogen bonds in hydration water

We studied the properties of the H-bond network of hydration water in the different layers around the lysozyme reported in Table 1. We start this analysis by calculating the probability distribution $P(\cos\gamma)$ of the angle γ between the two vectors joining the oxygen atom of a central water molecule with the oxygen atoms of two neighbor water molecules at a distance $d < 3.5$ Å, this distance corresponds to the first minimum of the water oxygen-oxygen RDF. The geometry of the angle γ for three molecules is shown in the top part of Fig. 3. This angle is a good probe of the local environment of a water molecule. If the water molecule is surrounded by four water molecules in a perfect tetrahedral structure the angle is $\gamma = 109.5^\circ$ ($\cos\gamma = -0.334$).

Fig. 3 shows the distributions of $\cos\gamma$ of hydration water in the different layers around the lysozyme and in bulk water at $T = 300$ K (upper panel) and $T = 250$ K (lower panel). The distributions are normalized to unit area.

At $T = 300$ K the distribution $P(\cos\gamma)$ of bulk water shows a broad peak with the maximum located at $\gamma \sim 104.5^\circ$ ($\cos\gamma = -0.250$), this peak is the signature of the nearly tetrahedral order present in liquid water at short range distance. At $T = 250$ K this peak becomes sharper, as the population of water molecules assuming tetrahedral structure is enhanced upon decreasing the temperature. Interestingly this angle corresponds to the experimental intermolecular angle HÔH of water, even though the SPC/E model has a fixed geometry with $\hat{O} = 109.47^\circ$. A secondary sharp peak is found at $\gamma \sim 53^\circ$ ($\cos\gamma = 0.6$) at both the temperatures, this peak corresponds to interstitial neighbor molecules. These findings are in agreement with previous results on SPC/E water at ambient conditions [31].

The behavior of the distributions $P(\cos\gamma)$ calculated for hydration water is shown in the same figure. We start by looking at the curve relative to the layer 0–4 Å, which shows at both the temperature the largest deviation with respect to bulk water. At $T = 300$ K, this distribution shows a broad peak centered at $\gamma \sim 109.5^\circ$, this is the tetrahedral peak at the correct tetrahedral angle. It is also evident by comparison with bulk water that there is a larger probability to find neighbor molecules at higher angles (look the shoulder at $\gamma \sim 140^\circ$) and correspondingly a depletion of the population assuming angle values $\gamma = 75$–90°. This effect is more evident at low temperature. The secondary sharp peak due to interstitial water is located at the bulk angle.

By looking at the layer 0–6 Å, we see that as soon as we include the second molecular layer of water in the analysis the tetrahedral peak moves closer to the value of bulk water, but at lower angle. This "jump" is plausibly due to the larger population of hydration water which assumes $\gamma \sim 75$–90° respect to the bulk. This population decreases as we move toward outer layers and correspondingly the tetrahedral peak increases and shifts toward the bulk value. The analysis on the water molecules belonging to outer shell shows that the more we move out from the protein the more hydration water recovers bulk-behavior, in fact the curves approach the bulk distribution progressively. The angle of interstitial water is completely unaffected by neither the environment (protein) nor the temperature.

Globally we can say that the distortions induced by the protein in the water H-bonds network are not much pronounced for hydration water. This is very similar to what happens to for water in hydrophobic confinement [32], in opposition to water in hydrophilic confinement, that completely suppresses the tetrahedral peak of water in the first 4 Å from the wall [31]. The largest deviation found for the shell 0–4 Å is related to the fact that this correspond the the first layer around the protein, therefore water molecules perturbed the most by the interaction with protein. We note in fact that water molecules belonging to this monolayer completely miss water neighbors on the protein side of the shell. On the other hand being the

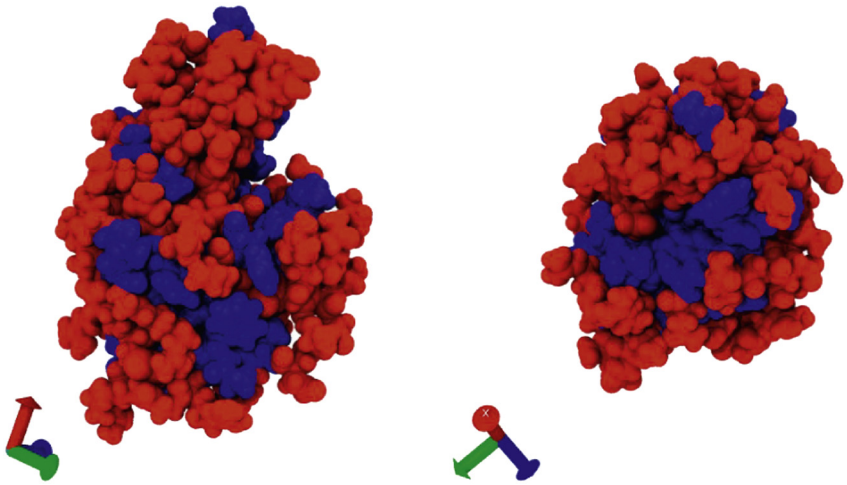

Fig. 1. Lysozyme in the Van der Waals representation, colored according to the hydrophobicity of its residues. Blue indicates hydrophobic residues, red indicates hydrophilic residues.

layer only 4 Å thick there is no room to develop a γ angle on the other side. Besides if we look at the RDF of hydrated sites, we see that no water molecules lie within ~2 Å from the protein due to the atomic repulsion. This mean that the layer 0–4 Å has a actual width of 2 Å, therefore we are basically analyzing a quasi 2-dimensional layer around the protein.

We now move to a coupled analysis focused on H-bonds. For the definition of an H-bond between two water molecules we adopted a criterion based on geometry, namely two water molecules are hydrogen bonded if the distance between their oxygen atoms is less than 3.5 Å and the angle $\hat{\text{HO}}\cdots\text{O}$ is less than or equal to 30°, where $\cdots$ indicates the H-bond. For SPC/E water, given the rigid structure of the molecule, these conditions hold to $r_{\text{HB}} < 2.7$ Å and $\beta > 140°$ (see the geometry). We analyzed the percentage of water molecules engaging n H-bonds with other water molecules in bulk water and in the different layers around the protein. The results are reported in Fig. 4 for $T = 300$ K and $T = 250$ K. There is no distinction between acceptor behavior and donor behavior, the total number of H-bonds is the sum of the two types. In none of the systems water molecules are observed to form $n > 7$ H-bonds.

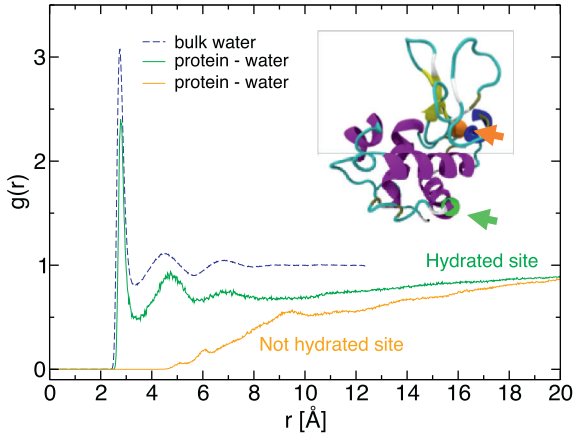

Fig. 2. RDF of water oxygen and a selected atom of the lysozyme, showing the difference between choosing an exposed/hydrated site/atom (green curve) and an inner/non-hydrated site/atom (orange curve). For comparison also the oxygen-oxygen RDF of bulk water is reported. The temperature is 300 K. In the inset, we show the location of the two selected sites of the lysozyme protein highlighted as balls superimposed to its secondary structure. The color of the arrow coincides with the color of the corresponding RDF.

At $T = 300$ K, water molecules in the layer 0–4 Å show a predominance to engage $n = 2$ H-bonds with the other water molecules of the layer. Moving to the layer 0–6 Å we find the maximum shifts to $n = 3$ H-bonds, and this behavior persists also in the layer 6–10 Å. Moving further away from the protein causes the increase of the fraction of water molecules engaging $n = 4$ H-bonds. We see that this happens in the layer 10–14 Å but the fractions relative to $n = 3,4$ are comparable. Bulk water mostly forms $n = 4$ H-bonds. Therefore in this solution we never recover the exact bulk water H-bonds distribution, not even for the layers further away from the protein.

Generally speaking the H-bonding behavior of bulk water is enhanced upon cooling. We see in fact that upon cooling bulk water the fraction of water forming $n = 4$ H-bonds grows at the expenses of other n values of H-bonds. For the hydration layers this happens only in the outer layer, being the $n = 4$ the maximum probability for that layer also at high temperature. For closer layers we see that this enhancement of H-bonds is reflected by the distribution shifting toward higher n values. So for the distribution in 6–10 Å the maximum shift to $n = 4$, in 0–6 Å it remains at $n = 3$ but the population at $n = 4$ grows at the expense of $n = 2$. In the 0–4 Å layer we see that even if the maximum remains at $n = 2$, the fraction of water molecules engaging $n = 3$ increases and becomes comparable with the fraction engaging $n = 2$ H-bonds.

In summary we see that water at the protein interface has a different H-bonds distribution, which is shifted toward lower n values and wider with respect to bulk water, with water forming mostly a total of three or two H-bonds. Also from the H-bonds point of view the 0–4 Å layer appears to be the more perturbed, and the mean number of H-bonds formed by a molecule is on average less than water in the outer layers and bulk water. This is also because about the 44.8% of these hydration water molecules in the 0–4 Å layers forms H-bonds with the protein atoms.

Table 1
Average number of water molecules, N_w, found in the layers around the lysozyme protein.

Layer	N_w (300 K)	N_w (250 K)
0–4 Å	604	648
0–6 Å	1076	1141
6–10 Å	2290	2410
10–14 Å	3878	4058

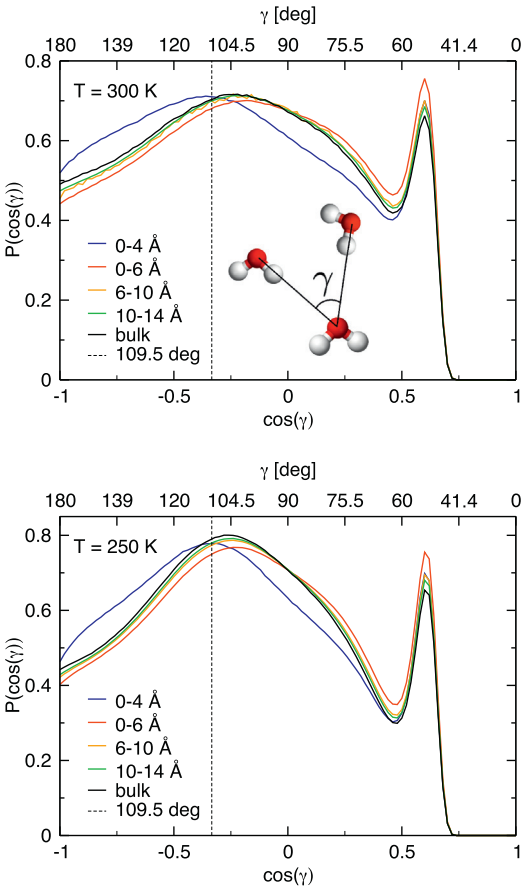

Fig. 3. Distribution $P(\cos\ \gamma)$ for bulk water and hydration water in different layers around the lysozyme at $T = 300$ K (upper panel) and $T = 250$ K (lower panel). The angle-scale for γ is shown in the upper x-axis of each plot. In the top panel the geometry of the angle γ is shown.

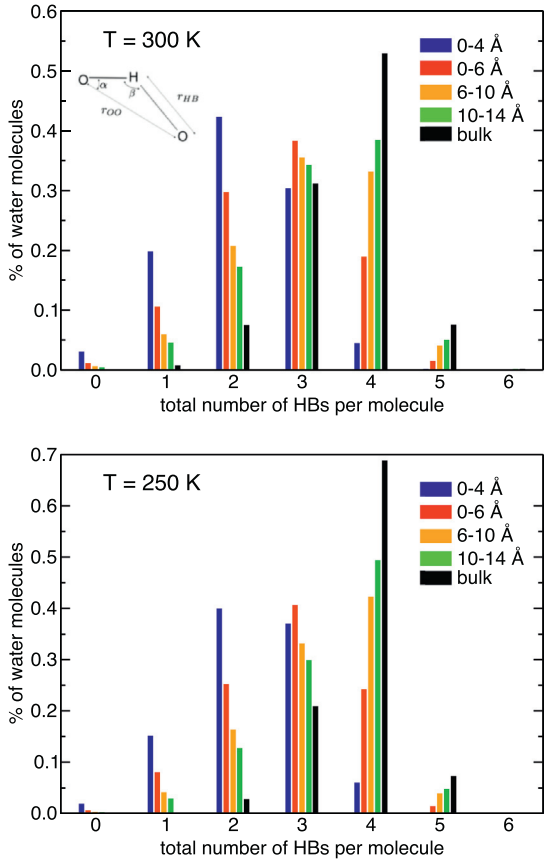

Fig. 4. Distributions of the population of water molecules engaging n H-bonds with another water molecules in the different layers around the lysozyme and in bulk water at $T = 300$ K (upper panel) and $T = 250$ K (bottom panel).

5. Translational dynamics of hydration water

5.1. Self intermediate scattering functions

Among the time correlation functions that can be calculated from MD trajectories to probe the translational single-particle dynamics the Self Intermediate Scattering Function (SISF) provides important information on the temporal dynamic regimes that a molecule undergoes during its motion. Besides it plays an important role in the field of physics of liquids because it is the correlation function that appears in the cross-section of neutron scattering experiments, which are widely used to characterized water and water-solutions. It plays an even more important role for supercooled water, being the SISF the central quantity of the Mode Coupling Theory (MCT) [33], the theory that at present describes the best water dynamics upon supercooling, in bulk [34-36], in confinement [37-40] and in solutions [41].

The SISF for water oxygen atoms is defined as

$$F_s(\vec{q},t) = \frac{1}{N}\left\langle \sum_{i=1}^{N} e^{i\vec{q}\bullet[\vec{r}_i(t)-\vec{r}_i(0)]} \right\rangle, \quad (1)$$

where N is the number of water molecules, $\vec{r}_i(t)$ is the position of the oxygen atom of the i-th water molecule at time t and $\vec{q}$ the transferred wave-vector. For an isotropic liquid, the SISF depends only on the module of $\vec{q}$, so we averaged over all the possible angles of the transferred wave-vector with fixed module to $|\vec{q}| = q_{max} = 2.25\ \text{Å}^{-1}$. This value corresponds to the first peak of the oxygen-oxygen structure factor of water where the MCT features are best evident [33]. We calculated the SISF for bulk water and for hydration water in the two closest layers 0–4 Å and 0–6 Å around the protein. For hydration water we correlate the positions of a water molecules at time t if and only if the water molecule moves within the layer during the time interval t, i.e. it does not exit the considered layer. Results are reported in Fig. 5 at two different temperatures of the systems, $T = 300$ K and $T = 250$ K.

All the curves show a fast decay at short time where they also coincide. In this regime a water molecule moves as a free particle, unperturbed by the interactions with other molecules and the motion is of ballistic type. The coincidence of the correlators calculated in the shells around the protein and in bulk water at a given temperature indicates that also hydration water molecules move freely and it shows that on the sub-100 fs time-scale water does not sense its local environment.

At a given temperature, the behavior of the SISFs in the different systems departs at few hundreds of femtoseconds. At $T = 300$ K for bulk water it is possible to see a sharp/fast transition from the ballistic motion to the diffusive motion and the correlation function decays to zero in about 5 ps. At $T = 250$ K, we can see the effect of being in supercooled regime: the transition from ballistic to the diffusive motion is characterized by a transient time regime where the SISF develops a plateau at about 500 fs before decaying to zero at about 30 ps. The plateau, which makes more clear the presence of

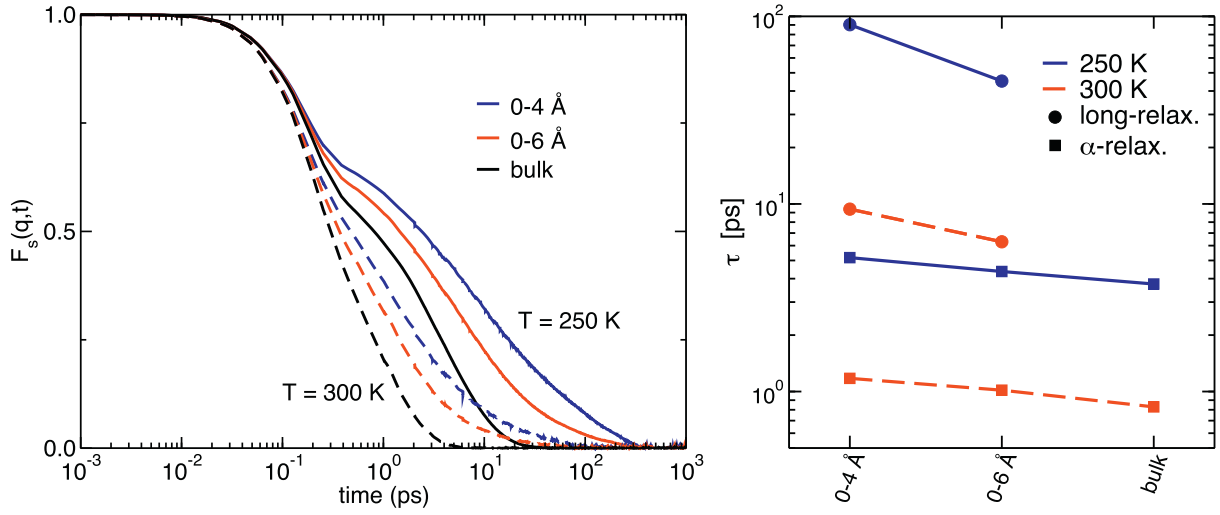

Fig. 5. Left panel: SISFs calculated for oxygen atoms in two different layers close to the protein (hydration water) and for bulk water at $T = 300\,\mathrm{K}$ and $T = 250\,\mathrm{K}$. Right panel: α-relaxation times and long-relaxation times extracted from the SISFs shown in the left panel.

two relaxation processes by visual inspection of the curve, is a peculiar feature of the supercooled regime and this behavior of the SISF is know as two step relaxation. To take into account both the relaxation processes, SISF of bulk water is modeled, according to [34,35], as

$$F_s(q,t) = (1-f_\alpha)e^{-(t/t_s)^2} + f_\alpha e^{-(t/t_\alpha)^{\beta\alpha}}, \tag{2}$$

where the gaussian term takes into account the first ballistic relaxation and the stretched exponential term the structural α-relaxation. The α-relaxation times extracted from the fit according to Eq. (2) of SISFs of bulk water at $T = 300\,\mathrm{K}$ and $T = 250\,\mathrm{K}$ are reported in Fig. 5.

We now move to SISFs of hydration water (Fig. 5). The correlations calculated for the monolayer 4 Å, is in general at a given temperature slower that the 6 Å, which is slower than that of bulk water at the same temperature. The main difference between bulk water and hydration water correlators appears at long time, whereas hydration water SISF shows an additional tail, which is not consistent with the MCT predictions of Eq. (2). The long-time tail is due to the presence of a third relaxation, the long-structural relaxation. This corresponds to adding a second stretched exponential function in Eq. (2) for the long-relaxation, leading to the following model for hydration water SISF [21]:

$$F_s(q,t) = (1-f_\alpha-f_l)\, e^{-(t/t_s)^2} + f_\alpha\, e^{-(t/t_\alpha)^{\beta\alpha}} + f_l\, e^{-(t/t_l)^{\beta_l}}. \tag{3}$$

In Fig. 5 we report the extracted relaxation times for hydration water at the two temperature investigated. At a given temperature, the τ_α is longer in the layer 0–4 Å and it decreases toward bulk value in the layer 0–6 Å. Is has been shown in fact that approximately above 10 Å the hydration water fully reaches bulk-like dynamics [22].

A similar trend is observed for the long relaxation time τ_l, being in the layer 0–4 Å higher than in the layer 0–6 Å. Nonetheless it shows a different dependence on the layer thickness with respect to the α-relaxation, in particular it appears more sensitive to the vicinity of the protein, as seen from the steeper jump between the two layers of τ_l with respect to the variation of τ_α. The long-relaxation is coupled with protein surface motion [23], therefore the dynamic coupling to the protein is expected to be at its maximum for those water molecules in direct contact with the protein surface, which are properly the first monolayer 0–4 Å.

5.2. Self Van Hove functions

The single-particle dynamics can be probed in real space through the Self van Hove Function (SVHF), defined as

$$G_s(\vec{r},t) = \frac{1}{N}\left\langle \sum_{i=1}^{N} \delta\left(\vec{r} - \vec{r}_i(t) + \vec{r}_i(0)\right)\right\rangle, \tag{4}$$

where N is the number of particle in the system. The SVHF gives the probability density that a particle experiences a displacement $\vec{r}$ in a time interval t. We calculated the SVHF for the oxygen atoms of water molecules in the layer 0–6 Å around the lysozyme and for bulk water.

In Fig. 6 the radial part of the SVHFs calculated for the hydration water at 300 K are reported in the short-time regime, namely in the range 100 fs–100 ps. The corresponding curves calculated for bulk water are shown in the upper part of the same figure.

The progression in time of the curves reflects the average motion of one water molecule. At short time the distribution is narrow and upon increasing time the maximum of the distribution moves toward larger distances, indicating that the molecule moves away from its starting position. The peak shift in time is accompanied by the broadening of the distribution. From the comparison of the two figures it is possible to see that the curves calculated for hydration water show a progressive slowing down with respect to the bulk phase: at a fixed time in fact the SVHF of hydration water shows the maximum always at shorter distance than the SVHFs of bulk water, for example at 10 ps the maxima are found at 1.5 Å for hydration water and at 3.0 Å for bulk water. This can be also seen by comparing the extension of the tails at longer time, where, for example, if we consider the motion during 100 ps we find that with a probability of 0.95 the motion of a water molecule inside the hydration layer is confined within a distance $d = 14\,\text{Å}$ from its starting position, while it is clear that in the case of bulk water this distance is larger by looking at the long tail of the curves: in this case in fact to reach a probability of 0.95 we have to extend the integration of the SVHF of

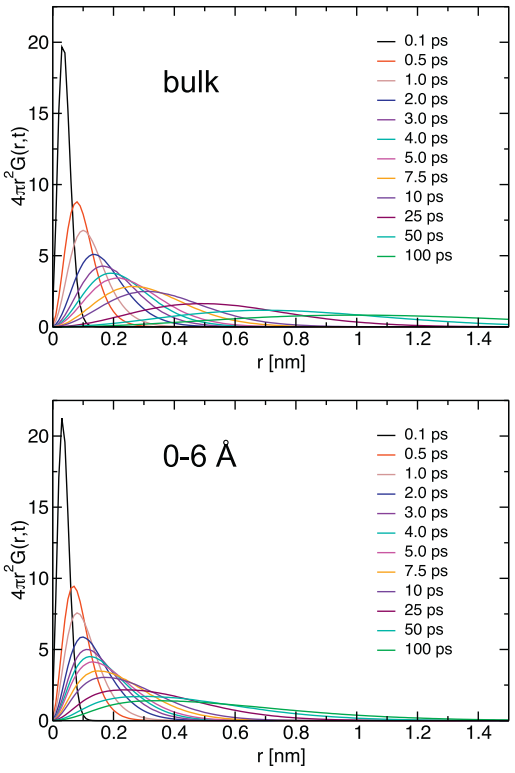

Fig. 6. Short time behavior of SVHFs. Upper panel: bulk water. Lower panel: hydration water. The temperature is 300 K.

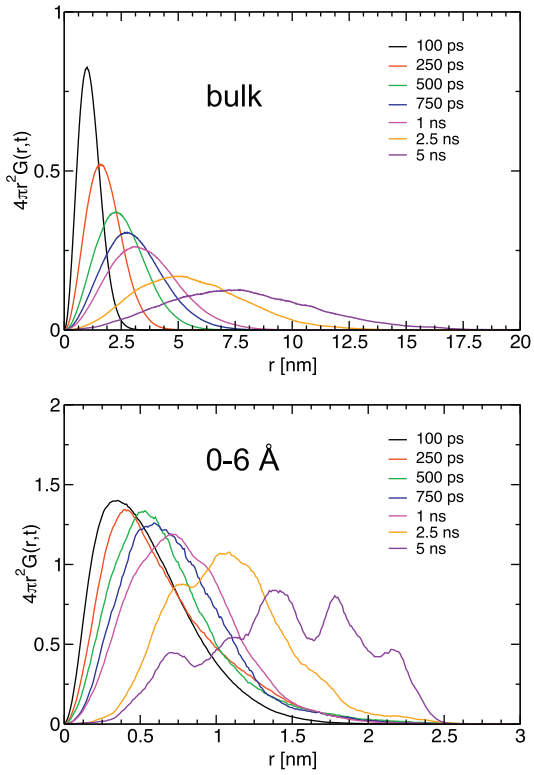

Fig. 7. Long time behavior of SVHFs. Upper panel: hydration water. Lower panel: Bulk water. The temperature is 300 K. Note the different x-scale of the panels.

bulk water up to 20 Å. From these curves we can therefore see that hydration water in the layer 0–6 Å has a slower dynamics compared to bulk water, as also shown by the SISFs.

In Fig. 7 the radial part of the SVHFs calculated for the hydration water at 300 K are reported in the long-time regime, namely in the range 100 ps–5 ns. The corresponding curves calculated for bulk water are shown in the upper part of the same figure. This slowing down of the dynamics is even more clear if we look at the SVHFs calculated in the long time regime. Note the different *r*-axis for the two panels.

The curves calculated for bulk continue to evolve in time, with their maximum moving toward larger distances and spreading out. The phenomenology of hydration water is very different in this timescale instead, and it can be summarized in the following way: (*i*) up to about 1 ns, the curves evolve in time, maintaining the dynamical features they show in the short time regime, i.e. every curve is a unimodal distribution which broadens and whose single maximum moves toward larger distance upon increasing the time. (*ii*) At 1 ns, the curve develops a shoulder at larger distance with respect to the position of its maximum, this shoulder is approximately located at ~9 Å. (*iii*) Above 1 ns the curves show multimodality. At 2.5 ns the SVHF of hydration water displays in fact two local maxima and a shoulder at larger distance, at 5.0 ns the curve develops five independent local maxima. (*iv*) The first maximum at 1, 2.5 and 5 ns does not move in time, meaning that a fraction of particles are trapped in some preferential location, probably protein sites. This phenomenology is complete absent in bulk water at $T = 300$ K.

The position of the maxima, r_{max}, at a given time corresponds to the largest density probability of finding a particle which experienced that displacement, therefore its behavior in time gives information on the type of motion. In Fig. 8 we show the position of the maxima of SVHFs for hydration water and for bulk water.

At 300 K it is known that SPC/E water enters the diffusive regime early in time and when the mean square displacement (MSD) reaches 0.1 nm^2 the dynamical regime is fully diffusive [34]. For our bulk it happens at above 5 ps and the MSD shows a linear dependence in time through an extracted diffusion coefficient

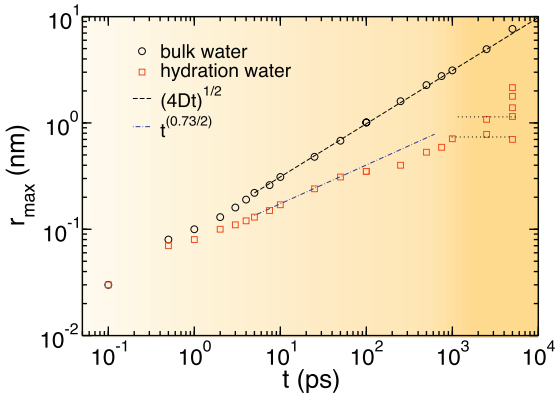

Fig. 8. Time behavior of the position of the maxima of SVHFs for hydration water and bulk water at 300 K. The darker yellow region is dominated by hopping processes due to the long-relaxation of hydration water where we observe multimodality in the SVHFs of hydration water.

$D = 2.40(\pm 0.01)\cdot 10^{-5}\,\mathrm{cm}^2/\mathrm{s}$. In diffusive regime the analytical expression for the SVHF is a gaussian given by

$$G_s(r,t) = \left(\sqrt[3]{4\pi D t}\right)^{-3/2} \exp\left(-\frac{r^2}{4Dt}\right). \quad (5)$$

Therefore the maximum of the radial part of Eq. (5) moves in time according to

$$r_{\max}(t) = \sqrt{4D}\; t^{1/2}, \quad (6)$$

i.e. as the square root of the MSD. We see from Fig. 8 that the peak maxima for bulk water nicely follow Eq. (6) as expected from the theory, confirming that the dynamics is diffusive. In the case of hydration water the motion is not diffusive also before the appearing of multiple-peaks, we see in fact that the dependence $t^{1/2}$ does not hold for hydration water. Besides at above 100 ps we see a change in the dynamical regime that we couldn't appreciate directly by looking at the curves: an additional slowing down of the dynamics is revealed by the change of the slope, which anticipates the appearing of multiple peaks/shoulders at 1 ns. The last dynamical regime of hydration water characterized by multimodality can be framed in the most general way into *hopping*-dynamics. In hopping-dynamics, in opposition to diffusive dynamics, the motion of a particles happens through non-infinitesimal jumps. A similar regime has been observed in cluster crystals of ultrasoft particles [42], where the slow dynamics happens through jumps between crystal sites.

For the hydration water confined in the layer around the protein with a thickness of 6 Å, the long-time motion is dominated by the displacement along the other two dimension, i.e. by the motion over the protein surface. The existence of preferred displacements can be related to transient trapping of water to protein-sites. This is consistent with the fact that water shows a spread distribution of residence times at protein sites, which goes from few ps up to thousands [5,43]. Water molecules could then escape from this environment through jumps: we see therefore a progressive appearance of new shoulders/peaks in the SVHF at the expense of the intensity of inner local maxima. For example the first local maximum in the curve at 1 ns persists as up to 5 ns, but its intensity decreases as some water molecules jump to other protein sites creating new local maxima in the SVHF at 2.5 ns and 5 ns.

As a final comment on our system, we think that the present hopping-mechanism has a different origin from the hopping phenomena which are matter of the extended MCT and regard the α-relaxation in bulk water [44]. In this case hopping activates density fluctuations of liquid water below the Widom line in correspondence of the fragile-to-strong transition of τ_α. MCT hopping phenomena are expected at much lower temperature in bulk water, when the SISF of water shows a long plateau regime right after the initial ballistic regime. MCT hopping phenomena restore the ergodicity of water that would be lost if the only relaxation mechanism was the structural relaxation of the cage of the nearest neighbors. Without them in fact there would be structural arrest.

We must mention that hopping phenomena of water have been observed in hydration water for example in concentrated carbohydrate-water solutions [45,46] already at ambient temperature, as in our case. But in the simulation works of Ref. [46] the oxygen-oxygen SVHFs show an in intense peak at distance within the first neighbors (trapped water) and secondary peaks coinciding with the positions of the first peaks of the oxygen-oxygen RDF (escaped water), which is the same phenomenology found at low temperature in bulk water [44]. We see in our case instead the hopping arising later in time, after the (sub)-diffusive motion which permits already to hydration water molecules to overcome the nearest-neighbors and the SVHF of hydration water show multiple peaks at very long distances than inter-particle ones (>10 Å). This further supports the idea they the distribution of the jump-lengths is probably connected to the topology of the surface and to the long-relaxation.

6. Summary and outlook

We used MD simulations to investigate structural and dynamical properties of the water surrounding the lysozyme protein. We show that water around hydrophilic sites organizes in well defined coordination shells, while it is almost excluded in the first 6 Å from buried/hydrophobic sites of the protein.

The structure and ordering of the water molecules in different layers around the protein are found to depend on the distance from the protein: the layer 0–4 Å from the protein experiences the largest distortion with respect to bulk water: even if the local order probed by the angle γ is nearly tetrahedral, water molecules tend to form less water-water H-bonds then in bulk. A fractions of these molecules is in fact also involved with protein-water H-bonds. Bulk-like behavior both for tetrahedral order and number of H-bonds, is progressively recovered up to the layer 10–14 Å from the protein, the furthest layer from the protein analyzed.

SISFs of water in the 0–4 Å and 0–6 Å layers show two distinct relaxations. The α-relaxation typical of many glass formers including water and a long-relaxation typical of water at protein interface. This last relaxation appears to be more sensitive to protein environment, being greatly slowed down moving closer to the protein, where the hydration molecules are the most influenced by the dynamic coupling with the protein.

By the study of SVHF of water in the layer 0–6 Å and monitoring its maximum in time, we show that water molecules move in the layer with sub-diffusive dynamics up to ~1 ns, when we observe a new peculiar dynamical regime: an hopping diffusion over distances quite larger than water-water nearest neighbor, the usual length-scale on which hopping phenomena allow relaxation in deeply supercooled liquids. We think that the mechanism that we observed here is due to jumps to particular sites of the protein which transiently trap water molecules.

Our interpretation deserves further investigation and a verification, for example, by connecting the jump-lengths to the protein topology and by comparing the temperature dependence of the observed phenomena with that of the long-relaxation of water and protein fluctuations. Future work will extend these last points.

References

[1] F. Franks, Water: A Matrix of Life, Second ed., The Royal Society of Chemistry, Cambridge, UK, 2000. https://doi.org/10.1039/9781847552341.
[2] J.A. Rupley, G. Careri, Protein hydration and function, Adv. Protein Chem. 41 (1991) 37–172. https://doi.org/10.1016/S0065-3233(08)60197-7.
[3] C. Rocchi, A.R. Bizzarri, S. Cannistraro, Water dynamical anomalies evidenced by molecular-dynamics simulations at the solvent-protein interface, Phys. Rev. E 57 (3) (1998) 3315–3325. https://doi.org/10.1103/PhysRevE.57.3315.
[4] A.R. Bizzarri, A. Paciaroni, S. Cannistraro, Glasslike dynamical behavior of the plastocyanin hydration water, Phys. Rev. E 62 (3) (2000) 3991–3999. https://doi.org/10.1103/PhysRevE.62.3991.
[5] A.R. Bizzarri, S. Cannistraro, Molecular dynamics of water at the protein-solvent interface, J. Phys. Chem. B 106 (26) (2002) 6617–6633. https://doi.org/10.1021/jp020100m.
[6] G. Cottone, S. Giuffrida, G. Ciccotti, L. Cordone, Molecular dynamics simulation of sucrose- and trehalose-coated carboxy-myoglobin, Proteins 59 (2) (2005) 291–302. https://doi.org/10.1002/prot.20414.
[7] F. Mallamace, C. Corsaro, D. Mallamace, H.E. Stanley, S.-H. Chen, Water and biological macromolecules, Liq. Polymorph. 152 (2013) 263. https://doi.org/10.1002/9781118540350.
[8] F. Mallamace, P. Baglioni, C. Corsaro, S.-H. Chen, D. Mallamace, C. Vasi, H.E. Stanley, The influence of water on protein properties, J. Chem. Phys. 141 (16) (2014) 165104. https://doi.org/10.1063/1.4900500.
[9] J.T. Titantah, M. Karttunen, Crossovers in supercooled solvation water: effects of hydrophilic and hydrophobic interactions, EPL Europhys. Lett. 110 (3) (2015) 38006. https://doi.org/10.1209/0295-5075/110/38006.

[10] M.-C. Bellissent-Funel, A.A. Hassanali, M. Havenith, R. Henchman, P. Pohl, F. Sterpone, D. van der Spoel, Y. Xu, A.E. García, Water determines the structure and dynamics of proteins, Chem. Rev. 116 (13) (2016) 7673–7697. https://doi.org/10.1021/acs.chemrev.5b00664.
[11] A. Kuffel, J. Zielkiewicz, Why the solvation water around proteins is more dense than bulk water, J. Phys. Chem. B 116 (40) (2012) 12113–12124. https://doi.org/10.1021/jp305172t.
[12] S.-H. Chen, L. Liu, E. Fratini, P. Baglioni, A. Faraone, E. Mamontov, M. Fomina, Observation of fragile-to-strong dynamic crossover in protein hydration water, Proc. Natl. Acad. Sci. U. S. A. 103 (24) (2006) 9012–9016. https://doi.org/10.1073/pnas.0602474103.
[13] M. Lagi, X.-q. Chu, C. Kim, F. Mallamace, P. Baglioni, S.-H. Chen, The low-temperature dynamic crossover phenomenon in protein hydration water: simulations vs experiments, J. Phys. Chem. B 112 (6) (2008) 1571–1575. https://doi.org/10.1021/jp710714j.
[14] G. Schirò, M. Fomina, A. Cupane, Communication: protein dynamical transition vs. liquid-liquid phase transition in protein hydration water, J. Chem. Phys. 139 (12) (2013) 121102. https://doi.org/10.1063/1.4822250.
[15] D.E. Khoshtariya, E. Hansen, R. Leecharoen, G.C. Walker, Probing protein hydration by the difference O-H (O-D) vibrational spectroscopy: interfacial percolation network involving highly polarizable water-water hydrogen bonds, J. Mol. Liq. 105 (1) (2003) 13–36. https://doi.org/10.1016/S0167-7322(03)00009-6.
[16] L. Zhang, L. Wang, Y.-T. Kao, W. Qiu, Y. Yang, O. Okobiah, D. Zhong, Mapping hydration dynamics around a protein surface, Proc. Natl. Acad. Sci. U. S. A. 104 (47) (2007) 18461–18466. https://doi.org/10.1073/pnas.0707647104.
[17] A. Paciaroni, E. Cornicchi, M. Marconi, A. Orecchini, C. Petrillo, M. Haertlein, M. Moulin, F. Sacchetti, Coupled relaxations at the protein-water interface in the picosecond time scale, J. R. Soc. Interface 6 Suppl 5 (2009) S635–S640. https://doi.org/10.1098/rsif.2009.0182.focus.
[18] L. Lupi, L. Comez, M. Paolantoni, D. Fioretto, B.M. Ladanyi, Dynamics of biological water: insights from molecular modeling of light scattering in aqueous trehalose solutions, J. Phys. Chem. B 116 (25) (2012) 7499–7508. https://doi.org/10.1021/jp301988f.
[19] L. Comez, L. Lupi, A. Morresi, M. Paolantoni, P. Sassi, D. Fioretto, More is different: experimental results on the effect of biomolecules on the dynamics of hydration water, J. Phys. Chem. Lett. 4 (7) (2013) 1188–1192. https://doi.org/10.1021/jz400360v.
[20] S. Perticaroli, D. Russo, M. Paolantoni, M.A. Gonzalez, P. Sassi, J.D. Nickels, G. Ehlers, L. Comez, E. Pellegrini, D. Fioretto, A. Morresi, Painting biological low-frequency vibrational modes from small peptides to proteins, Phys. Chem. Chem. Phys. 17 (17) (2015) 11423–11431. https://doi.org/10.1039/c4cp05388e.
[21] A. Magno, P. Gallo, Understanding the mechanisms of bioprotection: a comparative study of aqueous solutions of trehalose and maltose upon supercooling, J. Phys. Chem. Lett. 2 (9) (2011) 977–982. https://doi.org/10.1021/jz200256q.
[22] D. Corradini, E.G. Strekalova, H.E. Stanley, P. Gallo, Microscopic mechanism of protein cryopreservation in an aqueous solution with trehalose, Sci. Rep. 3 (2013) 1218. https://doi.org/10.1038/srep01218.
[23] G. Camisasca, M. De Marzio, D. Corradini, P. Gallo, Two structural relaxations in protein hydration water and their dynamic crossovers, J. Chem. Phys. 145 (4) (2016) 044503. https://doi.org/10.1063/1.4959286.
[24] S.-H. Chen, M. Lagi, X.-q. Chu, Y. Zhang, C. Kim, A. Faraone, E. Fratini, P. Baglioni, Dynamics of a globular protein and its hydration water studied by neutron scattering and MD simulations, Spectrosc. Int. J. 24 (1–2) (2010) 1–24. https://doi.org/10.3233/SPE-2010-0409.
[25] A.D. MacKerell, D. Bashford, M. Bellott, R.L. Dunbrack, J.D. Evanseck, M.J. Field, S. Fischer, J. Gao, H. Guo, S. Ha, D. Joseph-McCarthy, L. Kuchnir, K. Kuczera, F.T. Lau, C. Mattos, S. Michnick, T. Ngo, D.T. Nguyen, B. Prodhom, W.E. Reiher, B. Roux, M. Schlenkrich, J.C. Smith, R. Stote, J. Straub, M. Watanabe, J. Wiórkiewicz-Kuczera, D. Yin, M. Karplus, All-atom empirical potential for molecular modeling and dynamics studies of proteins, J. Phys. Chem. B 102 (18) (1998) 3586–3616. https://doi.org/10.1021/jp973084f.
[26] A.D. MacKerell, M. Feig, C.L. Brooks, Extending the treatment of backbone energetics in protein force fields: limitations of gas-phase quantum mechanics in reproducing protein conformational distributions in molecular dynamics simulations, J. Comput. Chem. 25 (11) (2004) 1400–1415. https://doi.org/10.1002/jcc.20065.
[27] H.J.C. Berendsen, J.R. Grigera, T.P. Straatsma, The missing term in effective pair potentials, J. Phys. Chem. 91 (24) (1987) 6269–6271. https://doi.org/10.1021/j100308a038.
[28] H.J.C. Berendsen, J.P.M. Postma, W.F. van Gunsteren, A. DiNola, J.R. Haak, Molecular dynamics with coupling to an external bath, J. Chem. Phys. 81 (8) (1984) 3684. https://doi.org/10.1063/1.448118.
[29] B. Hess, C. Kutzner, D. van der Spoel, E. Lindahl, GROMACS 4: algorithms for highly efficient, load-balanced, and scalable molecular simulation, J. Chem. Theory Comput. 4 (3) (2008) 435–447. https://doi.org/10.1021/ct700301q.
[30] N.C.J. Strynadka, M.N.G. James, Lysozyme revisited: crystallographic evidence for distortion of an N-acetylmuramic acid residue bound in site D, J. Mol. Biol. 220 (2) (1991) 401–424. https://doi.org/10.1016/0022-2836(91)90021-W.
[31] P. Gallo, M. Rapinesi, M. Rovere, Confined water in the low hydration regime, J. Chem. Phys. 117 (1) (2002) 369. https://doi.org/10.1063/1.1480860.
[32] P. Gallo, M. Rovere, Structural properties and liquid spinodal of water confined in a hydrophobic environment, Phys. Rev. E Stat. Nonlinear Soft Matter Phys. 76 (6) (2007) 061202. arXiv:0804.2964. https://doi.org/10.1103/PhysRevE.76.061202.
[33] W. Götze, Complex Dynamics of Glass-forming Liquids, Oxford University Press, New York, USA, 2009, 1–656. https://doi.org/10.1093/acprof:oso/9780199235346.001.0001.
[34] P. Gallo, F. Sciortino, P. Tartaglia, S.-H. Chen, Slow dynamics of water molecules in supercooled states, Phys. Rev. Lett. 76 (15) (1996) 2730–2733. https://doi.org/10.1103/PhysRevLett.76.2730.
[35] F. Sciortino, P. Gallo, P. Tartaglia, S.-H. Chen, Supercooled water and the kinetic glass transition, Phys. Rev. E 54 (6) (1996) 6331–6343.
[36] S.-H. Chen, P. Gallo, F. Sciortino, P. Tartaglia, Molecular-dynamics study of incoherent quasielastic neutron-scattering spectra of supercooled water, Phys. Rev. E 56 (4) (1997) 4231–4243. https://doi.org/10.1103/PhysRevE.56.4231.
[37] P. Gallo, M. Rovere, E. Spohr, Supercooled confined water and the mode coupling crossover temperature, Phys. Rev. Lett. 85 (20) (2000) 4317–4320. https://doi.org/10.1103/PhysRevLett.85.4317.
[38] P. Gallo, M. Rovere, E. Spohr, Glass transition and layering effects in confined water: a computer simulation study, J. Chem. Phys. 113 (24) (2000) 11324–11335. arXiv:0010147. https://doi.org/10.1063/1.1328073.
[39] P. Gallo, M. Rovere, S.-H. Chen, Dynamic crossover in supercooled confined water: understanding bulk properties through confinement, J. Phys. Chem. Lett. 1 (4) (2010) 729–733. https://doi.org/10.1021/jz9003125.
[40] P. Gallo, M. Rovere, S.-H. Chen, Water confined in MCM-41: a mode coupling theory analysis, J. Phys. Condens. Matter 24 (6) (2012) 064109. https://doi.org/10.1088/0953-8984/24/6/064109.
[41] P. Gallo, D. Corradini, M. Rovere, Fragile to strong crossover at the Widom line in supercooled aqueous solutions of NaCl, J. Chem. Phys. 139 (20) (2013) 204503. https://doi.org/10.1063/1.4832382.
[42] D. Coslovich, L. Strauss, G. Kahl, Hopping and microscopic dynamics of ultrasoft particles in cluster crystals, Soft Matter 7 (5) (2011) 2127. arXiv:1006.4982. https://doi.org/10.1039/c0sm00545b.
[43] G. Otting, E. Liepinsh, K. Wuthrich, Protein hydration in aqueous solution, Science 254 (5034) (1991) 974–980.
[44] M. De Marzio, G. Camisasca, M. Rovere, P. Gallo, Microscopic origin of the fragile to strong crossover in supercooled water: the role of activated processes, J. Chem. Phys. 146 (8) (2017) 084502.
[45] S. Magazù, G. Maisano, D. Majolino, P. Migliardo, A.M. Musolino, V. Villari, Diffusive properties of α,α-trehalose-water solutions, Prog. Theor. Phys. Suppl. 126 (0) (1997) 195–200. https://doi.org/10.1143/PTP.126.195.
[46] C.J. Roberts, P.G. Debenedetti, Structure and dynamics in concentrated, amorphous carbohydrate water systems by molecular dynamics simulation, J. Phys. Chem. B 103 (34) (1999) 7308–7318. https://doi.org/10.1021/jp9911548.